Article

J. Biol. Regul. Homeost. Agents. 2024; 38(5): 4263–4273
https://doi.org/10.23812/j.biol.regul.homeost.agents.20243805.338

Epigambogic Acid A from Gamboge Stalk Suppresses Non-Small Cell Lung Cancer Progression by Attenuating *DIRC1* Expression

Meng Wang[1,†], Binxian Jiang[2,†], Shuai Li[1], Kepu Du[1], Yadan Li[1], Fei Gao[1], Mengyu Gao[1], Bingqing Xu[3,*], Zhigang Zhou[1,*]

[1]Department of Radiology, The First Affiliated Hospital of Zhengzhou University, 450052 Zhengzhou, Henan, China
[2]Department of Emergency, Kunshan Hospital of Traditional Chinese Medicine, Kunshan Affiliated Hospital of Nanjing University of Chinese Medicine, 215399 Suzhou, Jiangsu, China
[3]Department of Geriatric, Affiliated Kunshan Hospital of Jiangsu University, 215399 Suzhou, Jiangsu, China
*Correspondence: bingqing5@sina.com (Bingqing Xu); Drzzg1966@126.com (Zhigang Zhou)
†These authors contributed equally.
Published: 1 May 2024

Background: Gamboge, a desiccating resin secreted by the gamboge tree, has shown potential anti-tumor effects. However, its impact and the underlying mechanisms against lung cancer are not well understood. This study explores the molecular mechanisms through which epigambogic acid A, a principal component of gamboge, inhibits the proliferation of non-small cell lung cancer (NSCLC) cells.

Methods: Normal lung epithelial cells BEAS-2B and human NSCLC cells were exposed to various concentrations of epigambogic acid A for 48 and 72 hours (h). Cell viability was assessed using a Cell Counting Kit-8 (CCK-8) assay, while colony formation ability was determined through a colony formation assay. Transwell invasion and migration assays were used to evaluate the cells' migratory and invasive capacities. Apoptotic processes were analyzed through flow cytometry, and expressions of associated biomarkers were investigated using Western blot. The Illumina HiSeq XTEN platform facilitated sequencing, while quantitative Real-time Polymerase chain reaction (qRT-PCR) quantified the expression of collagen type III alpha 1 chain (*COL3A1*) and disrupted in renal cancer 1 (*DIRC1*).

Results: Epigambogic acid A significantly inhibited NSCLC cell growth, with a 99.94% inhibition rate. It also reduced cell colony formation and suppressed the migratory and invasive abilities of NSCLC cells, and promoted apoptosis ($p < 0.05$). Transcriptome sequencing and analysis revealed that epigambogic acid A significantly decreased oncogene levels, including *DIRC1* and *COL3A1*. Furthermore, *DIRC1* was found to enhance colony formation and proliferation of NSCLC cells ($p < 0.05$).

Conclusions: This study demonstrates that epigambogic acid A effectively suppresses tumor growth in NSCLC by downregulating *DIRC1* expression. These findings suggest that epigambogic acid A is a potential therapeutic target for NSCLC treatment.

Keywords: Garcinia; anti-cancer; non-small cell lung cancer; epigambogic acid A; DIRC1; *COL3A1*

Introduction

Lung cancer remains the leading cause of cancer-related mortality worldwide, with non-small cell lung cancer (NSCLC) representing the majority of cases [1]. The incidence of Lung adenocarcinoma, the main pathological form of NSCLC, has shown a significant increase from 36.4% to 53.5%, highlighting its global predominance [2]. In recent years, with the in-depth understanding of genes and immune research, personalized therapy characterized by molecular targeted therapy and immunotherapy has become a promising modality for the treatment of NSCLC [3,4]. Although the therapy of NSCLC increased the survival of all ethnic groups by approximately 35%, patients with NSCLC still have a low 5-year life expectancy compared to those with other types of cancer [2,5]. Thus, there is an urgent need to develop novel anti-cancer treatments with reduced toxicity and strong efficacy [6,7].

Anti-tumor components from natural products have great potential for new drugs development. Several compounds, such as irinotecan [8,9], topotecan [10], and paclitaxel [11], have been developed from natural sources and have demonstrated remarkable anti-tumor efficacy. Gamboge, a yellow resin derived from the Garcinia tree, specifically from the trunk of the Garcinia hanburyi, has attracted attention for its broad-spectrum anti-cancer properties. Gambogic acid has broad-spectrum anti-tumor activity, including inducing autophagy [12] and apoptosis of tumor cells [13], blocking the cell cycle [14], inhibiting metastasis of cancer cells, inhibiting the angiogenesis of tumors and reversing multidrug resistance of tumor cells [15,16]. Epigambogic acid A, a standout compound iso-

Journal of
BIOLOGICAL REGULATORS
and Homeostatic Agents

lated from this resin, has emerged as a significant area of interest due to its potential in cancer therapy. Specifically extracted from the resin secreted by the gamboge stalk, the mechanism of action of epigambogic acid A in cancer treatment remains unclear.

The promising role of epigambogic acid A in cancer therapy is believed to be partly due to its ability to modulate gene expression related to tumor progression. Disrupted in renal cancer 1 (DIRC1) was initially identified to be closely correlated with the onset of kidney cancer. High expression of DIRC1 is observed in gastric cancer (GC), however, its expression is low in the testis, adult placenta, and skeletal muscle. DIRC1 is linked with the growth, penetration, and dissemination of GC cells [17,18]. However, the functional study of DIRC1 in lung cancer is limited. In this study, we extracted a novel compound, epigambogic acid A, from gamboge and conducted comprehensive *in vitro* research to reveal its functional role in NSCLC. Furthermore, we investigated the mechanism through which epigambogic acid A might influence the progression of NSCLC through its interaction with DIRC1.

Materials and Methods

Isolation of Epigambogic Acid A

The Garcinia resin was purchased from the Yunnan Jin-Fa Pharmaceutical Co. Ltd. (Kunming, China). The material was validated at Yunnan University of Traditional Chinese Medicine by Prof. Bin Qiu. A voucher specimen labelled with the code CHYX0629 has been formally submitted to Shenzhen University's School of Pharmaceutical Sciences (Shenzhen, China). A crude extract was obtained by ultrasonically treating 600 g of Garcinia resin (3 L × 1 h) at 25 °C with 95% EtOH. Subsequently, the extract was concentrated under low pressure. Altogether, 10 fractions (Fr.A–Fr.J) were produced by isolating the 390 g of extract on a silica gel column (200–300 mesh) and then eluted with a petroleum ether–acetone gradient (100:0→50:50). Fr.G (49.0 g) was partitioned into Fr.G.1–Fr.G.3 using MCI gel CHP 20P (Methanol/H_2O, 80%→100%). Fr.G.3 (10.0 g) underwent chromatography on a silica gel column and eluted with petroleum ether-Me_2CO (100:0→3:1) to generate six fractions (Fr.G.3.1–Fr.G.3.6). Fr.G.3.4 (500.0 mg) was subjected to Sephadex LH-20 chromatography (Methanol) followed by semi-preparative High Performance Liquid Chromatography (HPLC) (Methanol/H_2O containing 0.05% Trifluoroacetic Acid (TFA), 92%) to produce the compound epigambogic acid A (t_R = 22.2 min, 31.0 mg, flow rate: 3 mL/min).

Cell Culture and Transfection

The human NSCLC cell lines (PC9, HCC827, H1975, A549, and H1299) and the normal pulmonary epithelial cells BEAS-2B were procured from Guangzhou CellCook Biological Science and Technology Ltd. (Guangzhou, China). All cell lines were cultured in RPMI 1640 medium (11875168, Thermo Fisher Scientific, Waltham, MA, USA) supplemented with 10% fetal bovine serum (FBS; A5669501, Thermo Fisher Scientific, Waltham, MA, USA) and 1% penicillin-streptomycin-glutamine (10378016, Thermo Fisher Scientific, Waltham, MA, USA) at 37 °C, under standard conditions. BEAS-2B cells were kept in 5% CO_2 at 37 °C in BEGM medium (Lonza CC-3170, Guangzhou CellCook Biological Science and Technology Ltd., Guangzhou, China). The cells were assessed for mycoplasma contamination using the Applied Biosystems MycoSEQ detection kit (4460623, Thermo Fisher Scientific, Waltham, MA, USA), confirming negative results. Furthermore, STR identification was validated by Wuhan Zhishan Biotech Co. Ltd. (Wuhan, China), on 5th August, 2022.

For transfection, the cells in the logarithmic growth phase (2×10^5/mL) were cultured in 6-well plates, transfected at 70% confluency, and then incubated at 37 °C with 5% CO_2 for 6 h. The culture medium was replaced with a complete cell culture medium, and cells were allowed to grow for further 48 h. Afterwards, the transfection efficiency and subsequent analyses were conducted. GenePharma (Shanghai, China) provided empty vector (control vector) and overexpression of *DIRC1* (ov-*DIRC1*).

Cell Viability Assay

Approximately 3×10^3 cells/well of each cell line (PC9, A549, HCC827, H1975, H1299, and BEAS-2B) were cultured in 96-well plates followed by overnight incubation. Subsequently, the cells were treated with various concentrations of epigambogic acid A for 48 h and 72 h. For cell viability, Cell Counting Kit-8 (CCK-8) assay (CK04, Dojindo Laboratories, Kumamoto Prefecture, Japan) was performed according to the manufacturer's instruction. The half maximal inhibitory concentration (IC_{50}) was assessed and compared using GraphPad Prism (version 9.0, GraphPad Software, La Jolla, CA, USA).

Colony Formation Assay

PC9 and A549 cells (1×10^3 cells/well) were cultured in 6-well plates, treated with various concentrations (0, 0.5, 1, and 2 μM) of epigambogic acid A, and kept at 37 °C under humidified conditions for 10 days. Afterwards, the colonies were rinsed twice with phosphate buffer saline (PBS) and preserved using 4% paraformaldehyde at 25 °C for 30 min. Methanol was added to each well for 20 min. For colony staining, 0.1% crystal violet was applied for 2 h at 25 °C. The number of clones was elucidated using ImageJ software (version 1.8.0, National Institute of Health, Bethesda, MD, USA).

Transwell Invasion and Transwell Migration Assays

Initially, Matrigel (E6909, Merck, Burlington, MA, USA) was applied to the upper chamber of the transwell and

allowed to polymerize for 30 min at 37 °C. For transwell invasion assay, PC9 and A549 cells were cultured for 24 h in serum-free medium and then seeded (2×10^4 cells/well) in the upper chamber in FBS-free medium. In the lower chamber, medium enriched with 10% FBS was added, and the cells were cultured for 18 h at 37 °C. After this process, the cells were categorized into four groups according to the defined concentration of epigambogic acid A in the serum-free medium. Cells were preserved in 4% paraformaldehyde for 30 min, washed with PBS, and then incubated. After adding methanol to each well for 20 min, the cells were stained for 2 h at 25 °C using 0.1% crystal violet. The invading cells were quantified using light microscope (×200). The transwell migration assay was performed similarly, except that Matrigel was not added in the transwell chamber to examine the motility of cells. The number of cells was measured using ImageJ software (version 1.8.0, National Institute of Health, Bethesda, MD, USA).

Flow Cytometry

PC9 and A549 cells were cultured in a 6-cm dish and treated with a defined concentration of epigambogic acid A for 72 h. Subsequently, the cells were lysed, collected, and rinsed twice with ice-cold PBS. Afterwards, the cells were stained with propidium iodide (PI) and Annexin V-Fluorescein Isothiocyanate (FITC) for 15 min in the dark, using reagents obtained from the Annexin V-FITC/PI Cell Apoptosis Detection kit (AP101-100, Exxon (Beijing) Technology Co. Ltd., Beijing, China). Cell apoptosis was examined using a flow cytometer with the FAC Station data management system.

Western Blot

Proteins were quantified using the Bicinchoninic acid assay methods following cell lysis induced by RIPA buffer post treatment with epigambogic acid A (0, 0.5, 1, and 2 μM) for 72 h. Subsequently, the samples were transferred onto polyvinylidene fluoride membranes following electrophoresis on 10% SDS gel. The membrane was blocked by skim milk (5%) for 2 h and then incubated at 4 °C with the diluted (1:1000) primary antibodies: B-cell lymphoma-extra large (Bcl-XL) (#2764), Bcl-2-associated X protein (Bax) (#5023), mammalian target of rapamycin (mTOR) (#2983), phospho-mTOR (Ser2448) (#2971), Ak strain transforming (Akt) (#4691), phospho-Akt (Ser473) (#4060), and β-Actin (#4970). All these antibodies were acquired from Cell Signaling Technology, Danvers, MA, USA. Following three washes with Tris-buffered saline with Tween 20 (TBST), these membranes were kept for 1.5 h at 25 °C with the secondary HRP-labelled goat anti-rabbit antibody IgG (1:5000, Abcam Inc., Cambridge, MA, USA). For membranes development, the SuperSignal™ West Femto Maximum Sensitivity Substrate (34094, Thermo Fisher Scientific, Waltham, MA, USA) was used after TBST rinsing. The gray values of Western blot were semi-quantified by ImageJ software (version 1.8.0, National Institute of Health, Bethesda, MD, USA).

Transcriptome Sequencing

Following total RNA extraction, mRNA was isolated and cut into small fragments for cDNA synthesis using Oligo Magnetic Beads. The libraries were constructed following the guidelines provided by the manufacturer of the NEBNext UltraTM RNA Library Prep Kit (E7370L-96 reactions, New England Biolabs, Ipswich, MA, USA) designed for the Illumina system. The Illumina HiSeq XTEN platform was utilized across all sequences.

RNA Extraction and PCR Analysis

PC9 and A549 cells (3×10^5 cells/well) were cultured in 6-cm dish and treated with epigambogic acid A (0, 0.5, 1, and 2 μM) at 37 °C for 72 h. Total RNA of PC9 and A549 cells was collected using Trizol Reagent (15596-018, Thermo Fisher Scientific, Waltham, MA, USA). Afterwards, the acquired RNA was utilized for cDNA preparation as per instructions of the cDNA Synthesis Kit (RDTR, TransScript® One-Step gDNA Removal and cDNA Synthesis SuperMix, TransGen, Beijing, China). The primer pairs used in quantitative Real-time Polymerase chain reaction (qRT-PCR) were as follows: *DIRC1* forward, 5′-CAGGGACCTCGTTAATGGCT-3′ and reverse, 5′-CCGTTCAGACAGCTGACGTT-3′; collagen type III alpha 1 chain (*COL3A1*) forward, 5′-TTGAAGGAGGATGTTCCCATCT-3′ and reverse, 5′-ACAGACACATATTTGGCATGGTT-3′; glyceraldehyde-3-phosphate dehydrogenase (*GAPDH*) forward, 5′-GAAGGTGAAGGTCGGAGTC-3′ and reverse, 5′-GAAGATGGTGATGGGATTTC-3′.

The PCR settings were as follows: denaturation at 94 °C for 30 s, followed by 45 cycles at 94 °C for 5 s, 45 cycles at 60 °C for 30 s, and a final step at 4 °C. Internal control (β-actin) was used to normalize the tested genes. The analysis of fold changes in genes was carried out by the $2^{-\Delta\Delta Ct}$ method.

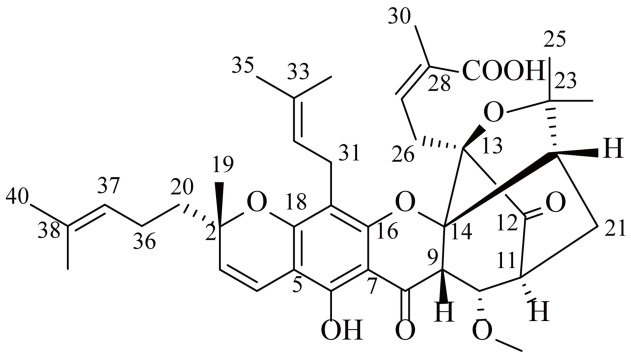

Fig. 1. The chemical structure of epigambogic acid A.

Journal of
BIOLOGICAL REGULATORS
and Homeostatic Agents

A

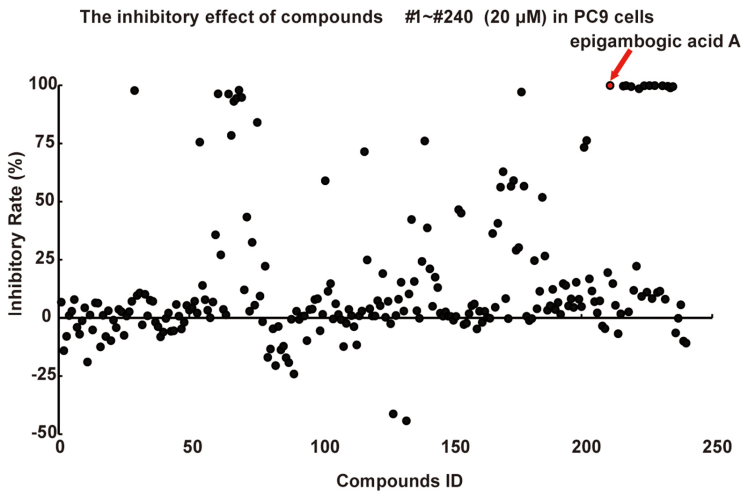

B

ID	Compound	Inhibitory Rate
#211	Epigambogic acid A	99.94
#226	TH-29	99.88
#228	TH-12	99.88
#217	TH-11	99.88
#224	AW-20	99.82
#231	TH-55	99.78
#216	TH-30	99.71
#233	TH-19	99.62
#235	TH-32	99.43
#219	TH-54	99.43
#234	TH-37	98.88
#222	TH-50	98.52
#69	D6-TR	97.89
#29	D6-CIS	97.79
#177	68-109-22	97.10
#61	TH-4	96.33
#65	EBSC-26b	96.29
#70	EBSC-26d	94.82
#68	EBSC-26a	94.36
#67	EBSC-26c	93.12
#76	DYLZ-13a	84.09
#66	LZ-22	78.46
#202	qfblz 96	76.30
#54	JKW-14	75.55
#201	qfblz 36	73.32
#178	qfblz 35	56.65
#118	X1812211	24.91

C

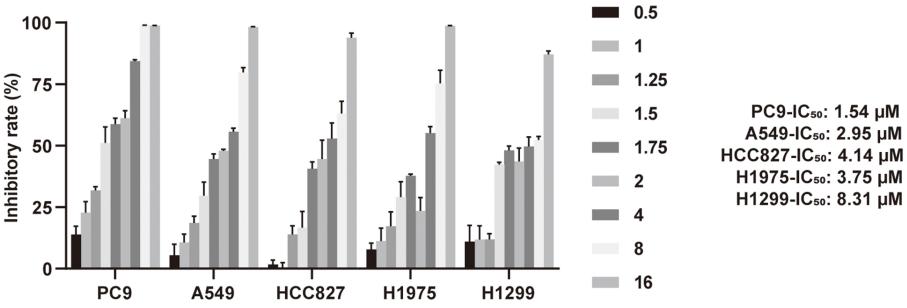

D

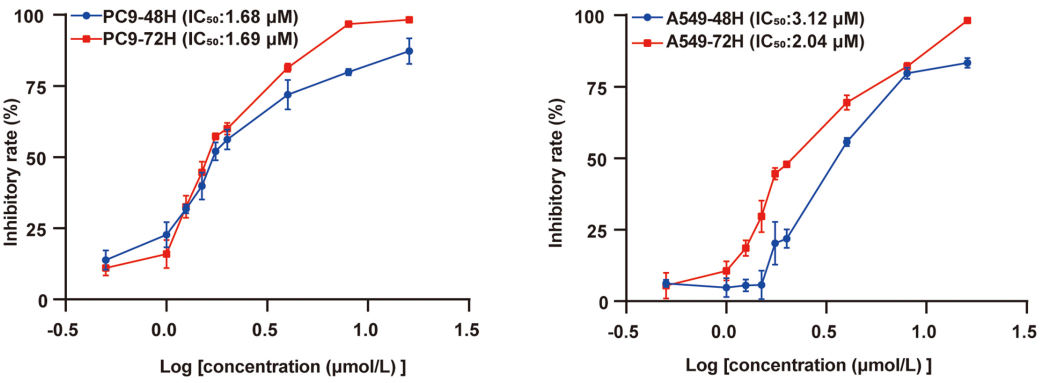

Fig. 2. Epigambogic acid A inhibited non-small cell lung cancer (NSCLC) cell's growth. (A) The inhibitory rates of compound #1–#240 extracted from Chinese herb tested in PC9 cells. Epigambogic acid A is shown in red. (B) The inhibitory rates of the top 27 compounds are shown. Epigambogic acid A ranked first. (C) Lung cancer cell lines H1975, PC9, HCC827, A549, and H1299 cells were treated with epigambogic acid A from 0.5 to 16 μM for 72 h, and the cell inhibitory rates were determined as described in the methods section. (D) The inhibitory rate curves of epigambogic acid A on PC9 and A549 cell lines for 48 h and 72 h. The data were reported in the Standard Deviation (SD) (N = 3). IC_{50}, half maximal inhibitory concentration.

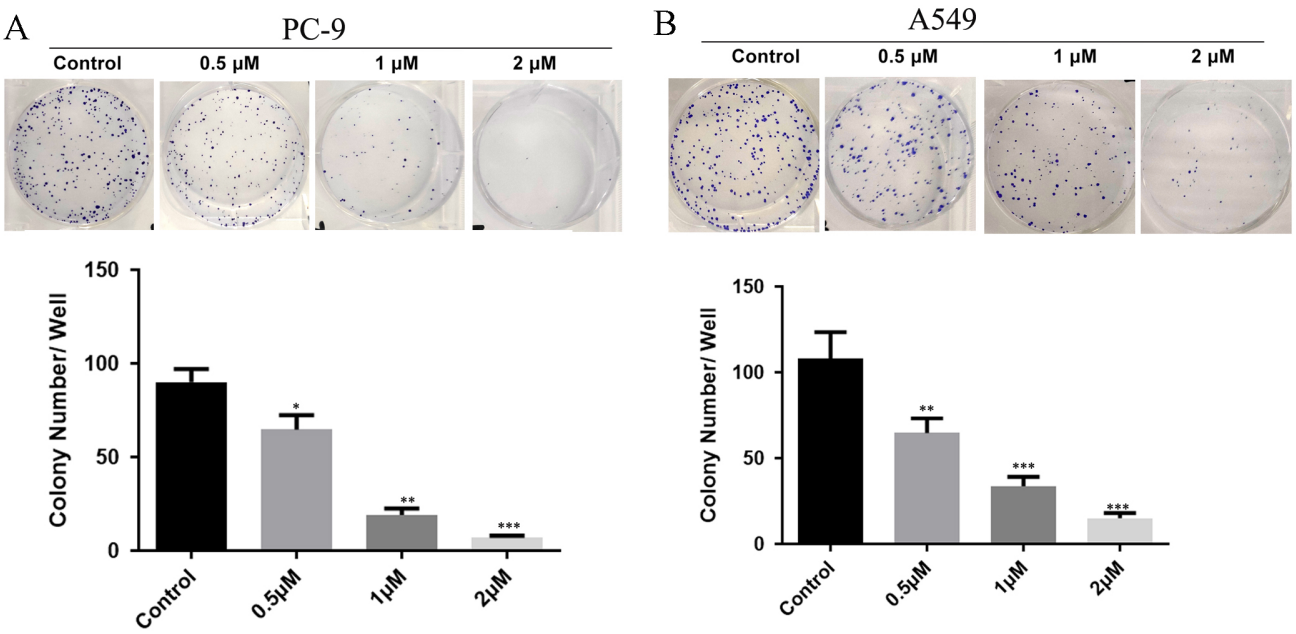

Fig. 3. Epigambogic acid A inhibited NSCLC cells colony formation. Changes of colony formation in PC9 (A) and A549 (B) cells after treatment with epigambogic acid A of 0.5, 1, and 2 μM. The bar chart on the right shows the number of colonies microscopically counted in 10 random fields. The data were reported in the SD of the mean. *$p < 0.05$, **$p < 0.01$, ***$p < 0.001$ (N = 3).

Statistical Analysis

All data were presented as mean ± Standard Deviation (SD). The GraphPad Prism 7.0 (version 9.0, GraphPad Software, La Jolla, CA, USA) software was employed to execute the statistical analyses. Student's *t*-test (between 2 groups) and one-way ANOVA with Bonferroni test (>2 groups) were employed. A threshold value of $p < 0.05$ was considered statistically significant.

Results

Structure Identification of Epigambogic Acid A

The structure of epigambogic acid A, including its relative configuration, was determined using spectroscopic data (Fig. 1). The ^{1}H and ^{13}C Nuclear Magnetic Resonance (NMR) data are consistent with those published findings [19] and listed in **Supplementary Table 1** and **Supplementary Fig. 1**. The purity of epigambogic acid A was examined by HPLC analysis [Agilent 1260 HPLC, SB-C18, 2.1 mm × 10 mm, i.d., 1.8 μm USA, MeCN-H_2O containing 0.05% TFA, 70%, t_R = 14.896 min, flow rate: 0.25 mL/min] (**Supplementary Fig. 2**).

Epigambogic Acid A Inhibited NSCLC Cell Growth

To examine the activity of Chinese herbal extracts in NSCLC cells, we screened 240 Chinese herbal extracts using the PC9 cell line and determined the cytotoxic effect of the compounds on the NSCLC cell growth. The data indicated that epigambogic acid A markedly inhibited PC9 cell growth at a concentration of 20 μM, and the inhibitory rate was 99.94% (Fig. 2A,B). Next, we examined the IC_{50} of epigambogic acid A in PC9, A549, HCC827, H1975, and H1299 cells by treating the cells with increasing concentrations of epigambogic acid A (0.5 to 16 μM) for 72 h. The IC_{50} was 1.54 ± 0.23, 2.95 ± 0.47, 4.14 ± 0.84, 3.75 ± 0.62, and 8.31 ± 1.57 μM, respectively, in these cells (Fig. 2C). Furthermore, we selected PC9 and A549 cells to further analyze the cytotoxicity of epigambogic acid A at 48 h and 72 h due to lower IC_{50} values. We found that the inhibitory rate was higher at the same concentration for 72 h (Fig. 2D). Consequently, 72 h was selected as the ideal duration for the subsequent examinations. We also observed the impact of epigambogic acid A on cell colony formation in PC9 and A549 cells. The findings revealed that the number of colonies was remarkably reduced with the increasing concentrations of epigambogic acid A (Fig. 3A,B). Based on these findings, epigambogic acid A appeared to impede NSCLC cell's proliferation.

Epigambogic Acid A Suppressed NSCLC Cell Migration and Invasion

The activity of epigambogic acid A on the NSCLC cell was assessed using transwell migration and invasion assays. The findings exhibited that epigambogic acid A inhibited the migration and invasion of PC9 and A549 cells in a dose-dependent manner (Fig. 4A,B). These outcomes demonstrated that epigambogic acid A remarkably reduced the NSCLC cells migration and invasion.

Journal of
BIOLOGICAL REGULATORS
and Homeostatic Agents

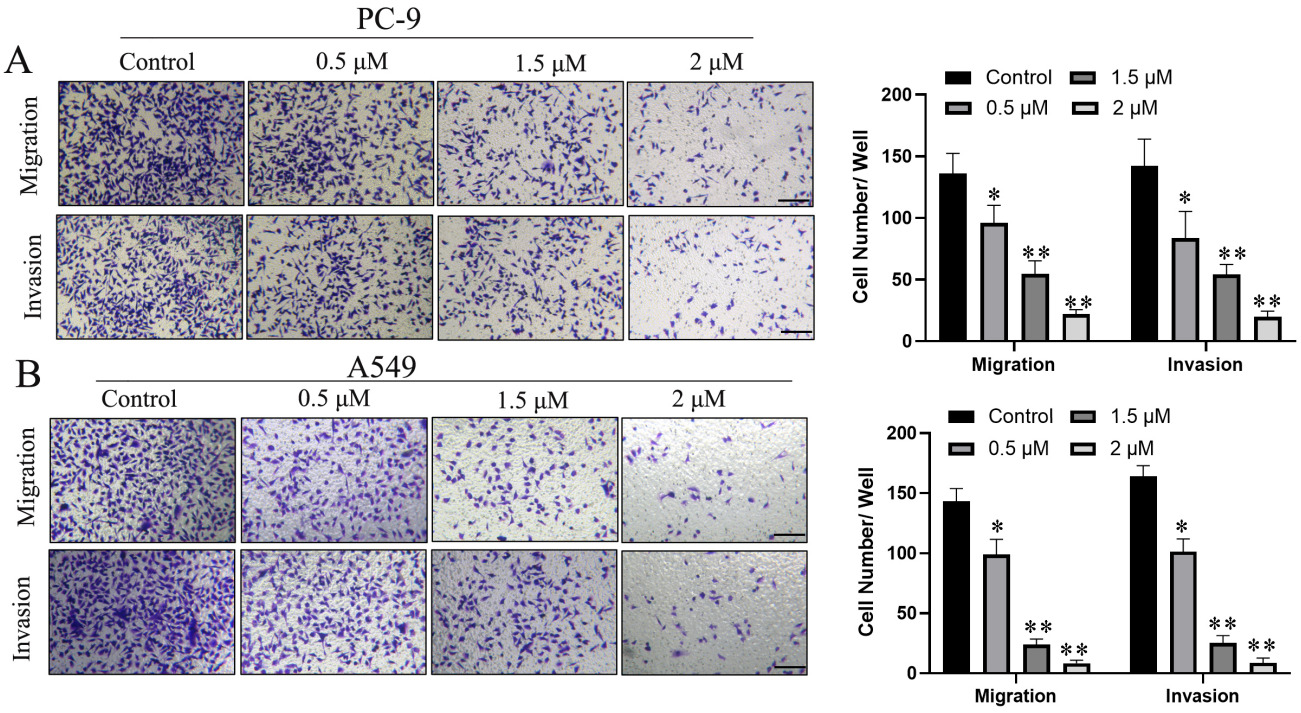

Fig. 4. Epigambogic acid A inhibited NSCLC cell migration and invasion. (A) After treatment with 0.5, 1, and 2 μM of epigambogic acid A, transwell was used to measure the effect of epigambogic acid A on PC-9 cell migration and invasion. Bar graphs show the number of migrated cells. (B) After treatment with 0.5, 1, and 2 μM of epigambogic acid A, transwell was used to measure the effect of epigambogic acid A on A549 cell migration and invasion. Bar graphs show the number of migrated cells. The data were reported in the SD. *$p < 0.05$; **$p < 0.01$ (N = 3). Scale bar is 100 μm.

Epigambogic Acid A Promoted Apoptosis of NSCLC Cells

Furthermore, we analyzed the impact of epigambogic acid A on apoptosis in NSCLC cells. The flow cytometry analysis showed that epigambogic acid A significantly induced apoptosis of PC9 and A549 cells (Fig. 5A,B). The levels of cell apoptosis-associated biomarkers, including Bax and Bcl-XL, were detected using Western blot assay. Epigambogic acid A notably upregulated the level of the cell apoptotic protein Bax and downregulated the level of the cell Bcl-XL (anti-apoptotic protein) in PC9 and A549 cells (Fig. 5C). We also explored the effect of epigambogic acid A on the level of mediators in the Ak strain transforming/mammalian target of rapamycin (Akt/mTOR) pathway. Western blot analysis exhibited that epigambogic acid A reduced the levels of P-Akt and phosphorylated-mTOR (p-mTOR), while the levels of total Akt and mTOR remained unchanged (Fig. 5D). These findings suggested that epigambogic acid A triggered cell apoptosis in NSCLC cells by suppressing the pathway of Akt/mTOR.

Epigambogic Acid A Downregulated DIRC1 Level in NSCLC Cells

To explore the mode of action of epigambogic acid A in tumorigenesis, we performed transcriptome sequencing. The analysis revealed differential expressions of 263 genes, and the expressions of 246 genes were changed with the treatment of epigambogic acid A (Fig. 6A). Finally, ten genes, including *COL3A1*, *DIRC1*, *MOGAT1*, *HMGCS2*, *SH3GL3*, *PCSK1N*, *FCRL5*, *AC011604.2*, *CALML5*, and *HOXA10-AS* were identified (Fig. 6B,C). To confirm these findings, *COL3A1* and *DIRC1* were further validated using qRT-PCR analysis in cells treated with increasing concentrations of epigambogic acid A. The findings confirmed that the levels of *COL3A1* and *DIRC1* were similar to the sequence of transcriptome (Fig. 6D).

Moreover, qRT-PCR was performed on the normal bronchial epithelial cell line BEAS-2B, as well as NSCLC cell lines PC9 and A549. The results indicated that *COL3A1* and *DIRC1* levels were substantially increased in the NSCLC cell lines relative to the normal cell line. These outcomes coincided with the findings retrieved from the the Cancer Genome Atlas (TCGA) database (Fig. 6E).

DIRC1 Promoted Cell Propagation in NSCLC Cells

In this study, we discovered the function of *DIRC1* in PC9 and A549 cells. After the overexpression of *DIRC1* (ov-*DIRC1*) compared with control vector (control group), the remarkable increase in colony formation was observed in PC9 and A549 cells (Fig. 7A,B). Further experiments on cell invasion and migration were performed, but no substan-

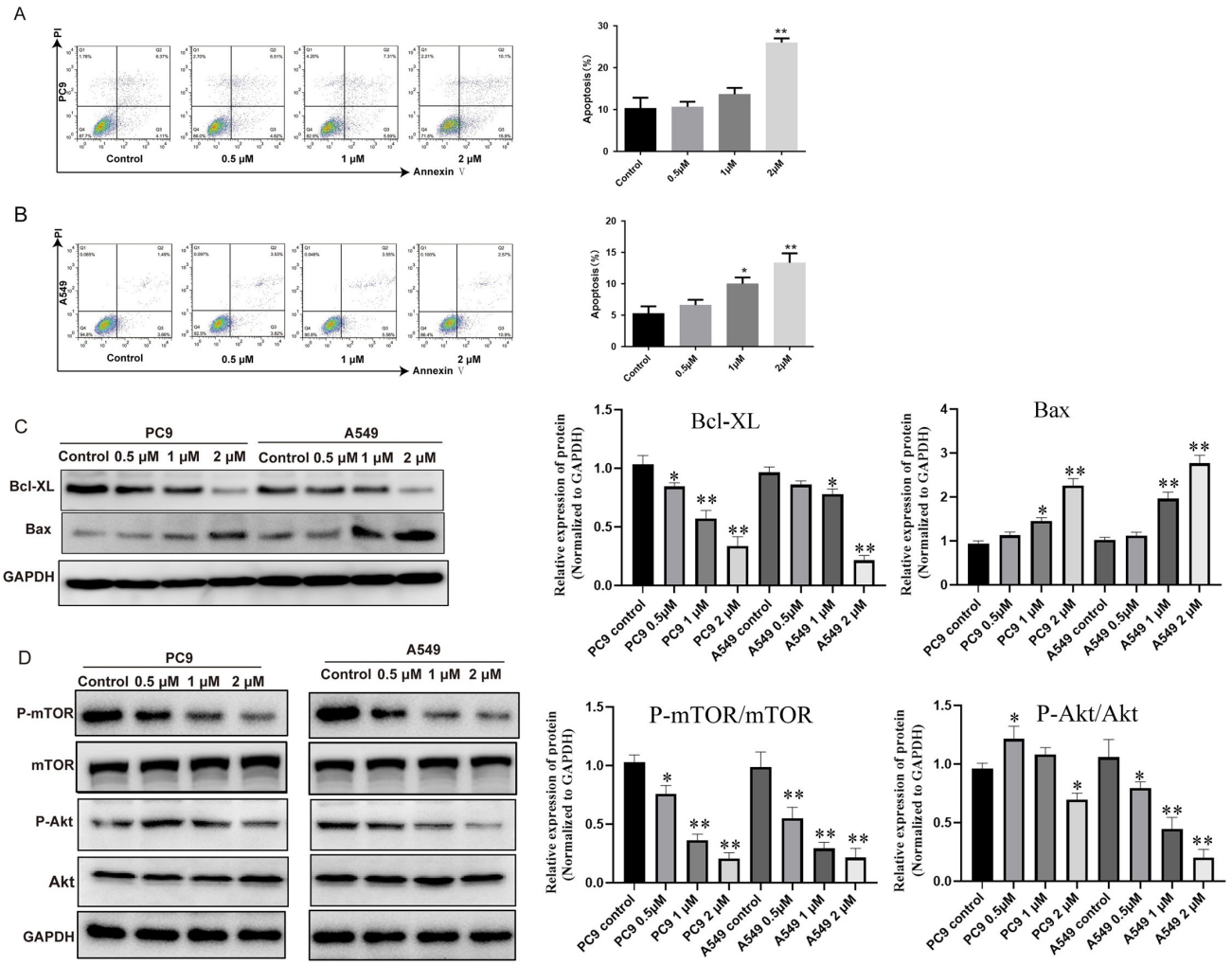

Fig. 5. Epigambogic acid A promoted apoptosis of NSCLC cells. (A,B) Cell apoptosis was examined by flow cytometry, and the apoptotic rate was shown in PC9 (A) and A549 (B). The concentrations of epigambogic acid A were 0.5, 1, and 2 μM. (C) Western blot analysis tested the protein expressions of B-cell lymphoma-extra large (Bcl-XL) and Bcl-2-associated X protein (Bax) on PC9 and A549 cells treated with epigambogic acid A at 0.5, 1, and 2 μM. (D) The protein levels of mammalian target of rapamycin (mTOR), phosphorylated-mTOR (p-mTOR), Ak strain transforming (Akt), and p-Akt were tested by Western blot on PC9 and A549 cells treated with epigambogic acid A at 0.5, 1, and 2 μM. The data were reported in the SD of the mean. $*p < 0.05$, $**p < 0.01$ (N = 3). GAPDH, glyceraldehyde-3-phosphate dehydrogenase.

tial differences were noted (**Supplementary Fig. 3**). These results showed that DIRC1 promoted NSCLC cells growth.

Discussion

In this study, we found that the compound epigambogic acid A, extracted from gamboge, effectively inhibits cell growth, dissemination, and penetration in NSCLC cells. Since there are always side effects associated with western medicine, traditional Chinese medicine is widely used in China due to its lower toxicity and beneficial effects, especially in the treatment of some cancers and recent Coronavirus Disease 2019 (COVID-19) disease [20]. It was reported that Kanglaite injection (a traditional Chinese medicine), combined with platinum-based chemotherapy, showed significantly higher efficacy compared to platinum-based chemotherapy alone in treating chronic lung cancer [21]. In addition, this combination therapy ameliorated the immunological function and reduced the toxicity resulting from chemotherapy [21]. As an alternative and complementary medicine for the management of colorectal cancer, the ethanolic extract of *T. kirilowii* inhibited cancer cell migration and invasion by decreasing the HIF-1 alpha/VEGF signaling pathway [22]. Our results revealed that epigambogic acid A had good efficacy in inhibiting cancer cell growth, migration, and invasion at low concentrations, which indicated that epigambogic acid A has an anti-tumor effect in NSCLC therapy.

Journal of
BIOLOGICAL REGULATORS
and Homeostatic Agents

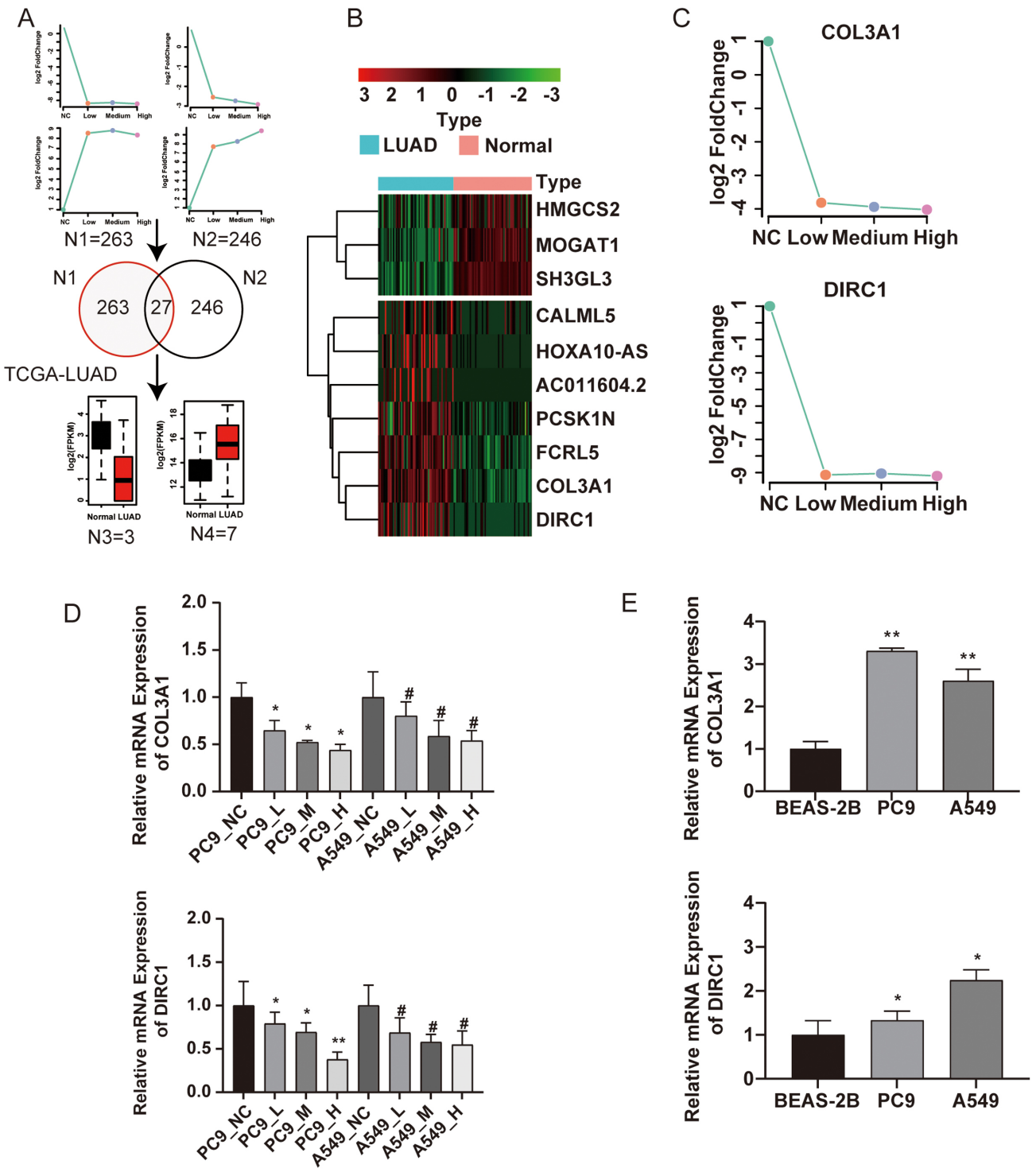

Fig. 6. Epigambogic acid A downregulated disrupted in renal cancer 1 (*DIRC1*) expression in NSCLC cells. (A) Screening differentially expressed genes in control and epigambogic acid A treated PC9 cells. (B) The thermogram showed ten genes in Lung adenocarcinoma, and the expression of three genes increased, and seven genes decreased significantly after treatment with epigambogic acid A ($log_2FC > 2$, $p < 0.05$). (C) Collagen type III alpha 1 chain (*COL3A1*) and *DIRC1* were decreased with the increase of epigambogic acid A concentration. The specific concentrations for low, medium, and high levels are 0.5 μM, 1 μM, and 2 μM, respectively. (D) Quantitative Real-time Polymerase chain reaction (qRT-PCR) detected the changes of *COL3A1* and *DIRC1* expression in PC9 and A549 with low, medium, and high concentrations of epigambogic acid A. The specific concentrations for low, medium, and high levels are 0.5 μM, 1 μM, and 2 μM, respectively. (E) Gene expression levels of *COL3A1* and *DIRC1* in BEAS-2B, PC9, and A549 were detected by RT-qPCR. The data were reported in SD. $*p < 0.05$, $**p < 0.01$, $^{\#}p < 0.05$ (N = 3). TCGA, the Cancer Genome Atlas.

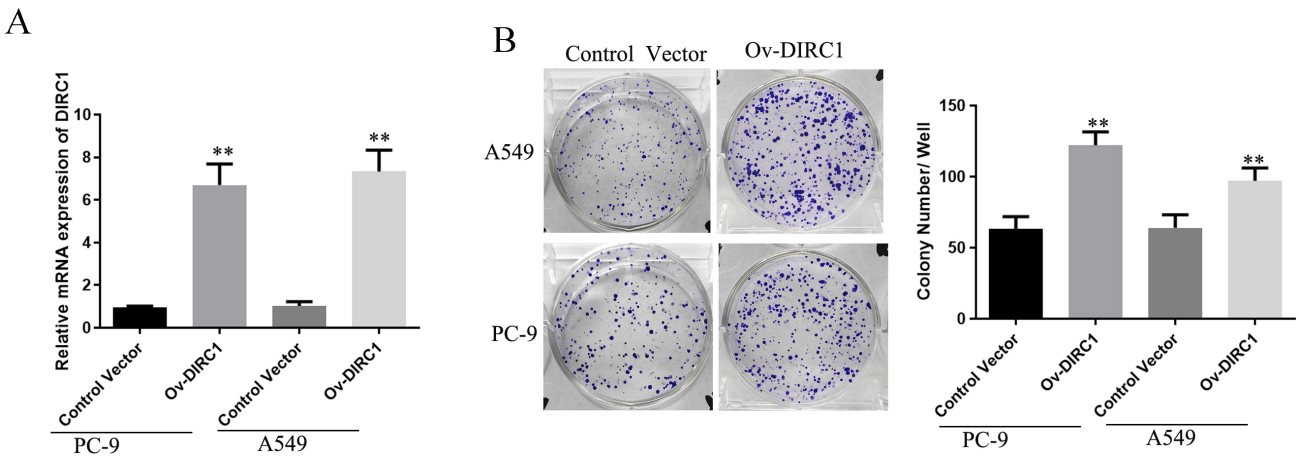

Fig. 7. Disrupted in renal cancer 1 (DIRC1) promoted cell growth in NSCLC cells. (A) RT-qPCR analysis of *DIRC1* mRNA level in PC9 and A549 cells after overexpressing *DIRC1*. (B) Changes of clonal formation after increased level of *DIRC1* in PC9 and A549 cell lines. The bar chart on the right shows the number of colonies microscopically counted in ten random fields. The data were reported in the SD of the mean. $^{**}p < 0.01$ (N = 3). ov-*DIRC1*, overexpression of *DIRC1*.

Recent findings have revealed that dysfunction in the Akt/mTOR signaling pathway is involved in tumorigenesis [23]. Aberrant activation of Akt/mTOR signaling inhibited cell apoptosis by upregulating anti-apoptosis-related proteins Bcl-XL and by downregulating apoptosis proteins Bax and caspase 3, eventually leading to the hyperproliferation of cancer cells [24,25]. Previous study revealed that the Akt/mTOR signaling pathway inhibited cancer cell apoptosis by regulating the level of apoptosis-related proteins [26]. The outcomes of this study indicated that epigambogic acid A induces cell apoptosis by suppressing the Akt/mTOR signaling pathway.

DIRC1 was identified as a breakpoint-spanning gene in a chromosomal translocation [18], which was associated with the progression of various cancers [17]. Previous study indicated a correlation between *DIRC1* overexpression and GC, as well as its contribution to the growth, invasion, and metastasis of GC cells [17]. Multiplex ligation-dependent probe amplification analysis in patients with aortic dilatation/dissection revealed the deletion of *DIRC1* and *COL3A1* genes [27]. *COL3A1*, encoding the collagen alpha-1 (III) chain, plays a crucial role in angiogenesis, cancer cell metastasis, and cell transformation [28]. In the present study, we observed that the levels of *COL3A1* and *DIRC1* were decreased in cells exposed to higher concentrations of epigambogic acid A. Furthermore, *DIRC1* was found to stimulate the expansion of NSCLC cells, which is similar to previous findings with GC [17]. The findings indicated that *DIRC1* may serve as a viable therapeutic target for NSCLC treatment.

In recent years, many researchers focused on developing and patenting new anti-cancer drugs for the treatment of various malignancies, including ovarian cancer [29], brain cancer [30], testicular tumors [31], thyroid cancer [32], and cutaneous melanoma [33]. The safety and efficacy of the anti-cancer compounds approved by the FDA were validated in animals and preclinical studies. There is a patent report about the advantages of administering low doses of paclitaxel over extended durations for breast cancer treatment. Paclitaxel is also very effective in the treatment of NSCLC [34]. Moreover, a recent patent reported that paclitaxel combined with anti-clusterin oligonucleotide increased the anti-cancer activity on NSCLC. Other related anti-cancer compounds also demonstrated efficacy for treating lung, gastric, and prostate cancers [35]. These anti-cancer compounds exhibit diverse effects on various types of tumors. These compounds affected tumor phenotypes, such as proliferation, apoptosis, and more, as we described in this article. Epigambogic acid A, as a single compound extracted from gambogic acid, has been extensively studied for its anti-cancer properties across various types of cancer, with remarkable effects on tumor cell apoptosis. According to another patent, other isolated products of gambogic acid resins also have therapeutic effects on various tumors. Moreover, given the low toxicity of Chinese herbal medicines and their efficacy in treating cancers and COVID-19 disease, more anti-cancer Chinese herbal medicines are required to be discovered and patented.

Conclusions

In conclusion, the results indicated that epigambogic acid A inhibits the signaling pathway of Akt/mTOR in NSCLC, thereby demonstrating its potential anti-tumor effects. Additionally, epigambogic acid A suppressed the expression of *DIRC1*, which promoted NSCLC cell growth. These findings provide scientific evidence that supports the use of epigambogic acid A as a complementary alternative medicine and suggest that *DIRC1* can be a possible therapeutic option for NSCLC.

Journal of
BIOLOGICAL REGULATORS
and Homeostatic Agents

Availability of Data and Materials

The data supporting our findings can be found in the article. All of the data generated in this study are available on request.

Author Contributions

MW and BXJ designed and performed the experiments; KPD, MYG, FG and ZGZ collected the data; SL, YDL and BQX performed the statistical analysis; FG and ZGZ wrote the manuscript; all authors contributed to editorial changes in the manuscript; all authors read and approved the final manuscript; all authors have participated sufficiently in the work and agreed to be accountable for all aspects of the work.

Ethics Approval and Consent to Participate

Not applicable.

Acknowledgment

Not applicable.

Funding

This research received no external funding.

Conflict of Interest

The authors declare no conflict of interest.

Supplementary Material

Supplementary material associated with this article can be found, in the online version, at https://doi.org/10.23812/j.biol.regul.homeost.agents.20243805.338.

References

[1] Siegel RL, Miller KD, Jemal A. Cancer statistics, 2020. CA: A Cancer Journal for Clinicians. 2020; 70: 7–30.

[2] Blandin Knight S, Crosbie PA, Balata H, Chudziak J, Hussell T, Dive C. Progress and prospects of early detection in lung cancer. Open Biology. 2017; 7: 170070.

[3] Hirsch FR, Suda K, Wiens J, Bunn PA, Jr. New and emerging targeted treatments in advanced non-small-cell lung cancer. Lancet. 2016; 388: 1012–1024.

[4] Song H, Liu D, Dong S, Zeng L, Wu Z, Zhao P, *et al*. Epitranscriptomics and epiproteomics in cancer drug resistance: therapeutic implications. Signal Transduction and Targeted Therapy. 2020; 5: 193.

[5] Howlader N, Forjaz G, Mooradian MJ, Meza R, Kong CY, Cronin KA, *et al*. The Effect of Advances in Lung-Cancer Treatment on Population Mortality. The New England Journal of Medicine. 2020; 383: 640–649.

[6] Wang Y, Zhang Q, Chen Y, Liang CL, Liu H, Qiu F, *et al*. Antitumor effects of immunity-enhancing traditional Chinese medicine. Biomedicine & Pharmacotherapy. 2020; 121: 109570.

[7] Portugal J. Challenging transcription by DNA-binding antitumor drugs. Biochemical Pharmacology. 2018; 155: 336–345.

[8] Bailly C. Irinotecan: 25 years of cancer treatment. Pharmacological Research. 2019; 148: 104398.

[9] Frampton JE. Liposomal Irinotecan: A Review in Metastatic Pancreatic Adenocarcinoma. Drugs. 2020; 80: 1007–1018.

[10] Goto K, Ohe Y, Shibata T, Seto T, Takahashi T, Nakagawa K, *et al*. Combined chemotherapy with cisplatin, etoposide, and irinotecan versus topotecan alone as second-line treatment for patients with sensitive relapsed small-cell lung cancer (JCOG0605): a multicentre, open-label, randomised phase 3 trial. The Lancet. Oncology. 2016; 17: 1147–1157.

[11] Abu Samaan TM, Samec M, Liskova A, Kubatka P, Büsselberg D. Paclitaxel's Mechanistic and Clinical Effects on Breast Cancer. Biomolecules. 2019; 9: 789.

[12] Wang H, Zhao Z, Lei S, Li S, Xiang Z, Wang X, *et al*. Gambogic acid induces autophagy and combines synergistically with chloroquine to suppress pancreatic cancer by increasing the accumulation of reactive oxygen species. Cancer Cell International. 2019; 19: 7.

[13] Su SC, Chen YT, Hsieh YH, Yang WE, Su CW, Chiu WY, *et al*. Gambogic Acid Induces HO-1 Expression and Cell Apoptosis through p38 Signaling in Oral Squamous Cell Carcinoma. The American Journal of Chinese Medicine. 2022; 50: 1663–1679.

[14] Wang X, Chen Y, Han QB, Chan CY, Wang H, Liu Z, *et al*. Proteomic identification of molecular targets of gambogic acid: role of stathmin in hepatocellular carcinoma. Proteomics. 2009; 9: 242–253.

[15] Qiang L, Yang Y, You QD, Ma YJ, Yang L, Nie FF, *et al*. Inhibition of glioblastoma growth and angiogenesis by gambogic acid: an in vitro and in vivo study. Biochemical Pharmacology. 2008; 75: 1083–1092.

[16] Wan L, Zhang Q, Wang S, Gao Y, Chen X, Zhao Y, *et al*. Gambogic acid impairs tumor angiogenesis by targeting YAP/STAT3 signaling axis. Phytotherapy Research. 2019; 33: 1579–1591.

[17] Li Z, Yang AJ, Wei FM, Zhao XH, Shao ZY. Significant association of DIRC1 overexpression with tumor progression and poor prognosis in gastric cancer. European Review for Medical and Pharmacological Sciences. 2018; 22: 8682–8689.

[18] Druck T, Podolski J, Byrski T, Wyrwicz L, Zajaczek S, Kata G, *et al*. The DIRC1 gene at chromosome 2q33 spans a familial RCC-associated t(2;3)(q33;q21) chromosome translocation. Journal of Human Genetics. 2001; 46: 583–589.

[19] Chen Y, He S, Tang C, Li J, Yang G. Caged polyprenylated xanthones from the resin of Garcinia hanburyi. Fitoterapia. 2016; 109: 106–112.

[20] Yang Y, Islam MS, Wang J, Li Y, Chen X. Traditional Chinese Medicine in the Treatment of Patients Infected with 2019-New Coronavirus (SARS-CoV-2): A Review and Perspective. International Journal of Biological Sciences. 2020; 16: 1708–1717.

[21] Huang X, Wang J, Lin W, Zhang N, Du J, Long Z, *et al*. Kanglaite injection plus platinum-based chemotherapy for stage III/IV non-small cell lung cancer: A meta-analysis of 27 RCTs. Phytomedicine. 2020; 67: 153154.

[22] Park SM, Jeon SK, Kim OH, Ahn JY, Kim CH, Park SD, *et al*. Anti-tumor effects of the ethanolic extract of *Trichosanthes kirilowii* seeds in colorectal cancer. Chinese Medicine. 2019; 14: 43.

[23] Lim HJ, Crowe P, Yang JL. Current clinical regulation of PI3K/PTEN/Akt/mTOR signalling in treatment of human cancer. Journal of Cancer Research and Clinical Oncology. 2015; 141: 671–689.

[24] Yu J, Wang W, Yao W, Yang Z, Gao P, Liu M, *et al*. Gambogic acid affects ESCC progression through regulation of PI3K/AKT/mTOR signal pathway. Journal of Cancer. 2020; 11: 5568–5577.

[25] Zhou J, Jiang YY, Chen H, Wu YC, Zhang L. Tanshinone I attenuates the malignant biological properties of ovarian cancer by inducing apoptosis and autophagy via the inactivation of PI3K/AKT/mTOR pathway. Cell Proliferation. 2020; 53: e12739.
[26] Zhang J, Xie T. Ghrelin inhibits cisplatin-induced MDA-MB-231 breast cancer cell apoptosis via PI3K/Akt/mTOR signaling. Experimental and Therapeutic Medicine. 2020; 19: 1633–1640.
[27] Meienberg J, Rohrbach M, Neuenschwander S, Spanaus K, Giunta C, Alonso S, *et al*. Hemizygous deletion of COL3A1, COL5A2, and MSTN causes a complex phenotype with aortic dissection: a lesson for and from true haploinsufficiency. European Journal of Human Genetics. 2010; 18: 1315–1321.
[28] Kuivaniemi H, Tromp G. Type III collagen (COL3A1): Gene and protein structure, tissue distribution, and associated diseases. Gene. 2019; 707: 151–171.
[29] Shafabakhsh R, Asemi Z. Quercetin: a natural compound for ovarian cancer treatment. Journal of Ovarian Research. 2019; 12: 55.
[30] Shah V, Kochar P. Brain Cancer: Implication to Disease, Therapeutic Strategies and Tumor Targeted Drug Delivery Approaches. Recent Patents on Anti-Cancer Drug Discovery. 2018; 13: 70–85.
[31] Chieffi P, De Martino M, Esposito F. New Anti-Cancer Strategies in Testicular Germ Cell Tumors. Recent Patents on Anti-Cancer Drug Discovery. 2019; 14: 53–59.
[32] Elia G, Ferrari SM, Ragusa F, Paparo SR, Mazzi V, Ulisse S, *et al*. Advances in pharmacotherapy for advanced thyroid cancer of follicular origin (PTC, FTC). New approved drugs and future therapies. Expert Opinion Pharmacotherapy. 2022; 23: 599–610.
[33] Basile D, Lisanti C, Pizzichetta MA, Baldo P, Fornasier G, Lo Re F, *et al*. Safety Profiles and Pharmacovigilance Considerations for Recently Patented Anticancer Drugs: Cutaneous Melanoma. Recent Patents on Anti-cancer Drug Discovery. 2019; 14: 203–225.
[34] Wei L, Miller DD, Subhash C, Kumar KV, Wang Q, inventor; Griffith H, assignee. Compounds for treatment of pancreatic cancer. USA. AU2019270091. 24 December 2020.
[35] Pui-Kwong C, Sung MM, inventor. Natural and synthetic compounds for treating cancer and other diseases. USA. AU2012284244A1. 9 May 2013.